Independent Emission of Neutral and Charged Clusters In High-Energy Hadron Collisions*

Charles B. Chiu and Kuo-Hsiang Wang
Center for Particle Theory, University of Texas, Austin, Texas 78712
(Received 25 June 1973)

A general formalism for the simultaneous emission of neutral and charge clusters is considered. For application, we study in detail a typical two-component model based on cluster emissions. We parameterize the diffractive component by a $\pi\sigma$ scheme and the nondiffractive component by a πB scheme. In the nondiffractive component, the strength parameters for the emission of both π and B are found empirically to be linear in $\ln p_{\rm Lab}$ in reminiscence of the expectation of a multiperipheral model. Furthermore, the direct pion emission is found to dominate in the low-energy region (20–30 GeV/c), while beyond 100 GeV/c, the B emission becomes more important. This indicates that the clustering effect becomes more and more important as the energy increases. The charge multiplicity distribution and the average π^0 multiplicity at fixed π^- number $\langle n_0\rangle_-$ vs n_-, predicted by the model are in good agreement with the data. Asymptotically the separation of the two components becomes noticeable at around 1000–1500 GeV/c and the prediction for $\langle n_0\rangle_-$ vs n_- at 1500 GeV/c is essentially the same as that at 205 GeV/c. Most features enumerated here appear to be quite general properties of two-component models involving the direct independent emission of pions and other clusters, insensitive to the specific πB scheme assumed.

I. INTRODUCTION

It is well known that in high-energy collisions, pion multiplicity distributions generally deviate from a simple Poisson distribution—a characteristic distribution predicted by uncorrelated pion emissions. Various suggestions have been advanced to account for such a deviation. These are essentially of the following three categories: (1) a two-component picture, (2) independent emission of resonances (or clusters), and (3) effects of conservation of charge. We recall briefly these suggestions. For the first case, the two components are the "diffractive" and the "nondiffractive" components.[1] The former is contributed by the "diffractive dissociation" events, which are believed to have an energy-independent multiplicity distribution with a relatively low average multiplicity. We denote as usual the average multiplicity $f_1=\langle n\rangle$, and the correlation parameter $f_2=\langle n(n-1)\rangle-\langle n\rangle^2$ (for a Poisson case, $f_2=0$), and the branching ratio of the diffractive component, λ. Assuming the multiplicity distribution is given by an incoherent sum of this component (d) and the rest, which is the nondiffractive component (nd), the resultant correlation parameter is

$$f_2=\lambda f_2^{\rm d}+(1-\lambda)f_2^{\rm nd}+\lambda(1-\lambda)(f_1^{\rm d}-f_1^{\rm nd})^2. \qquad (1.1)$$

With $f_1^{\rm d}\approx$ constant and $f_1^{\rm nd}\propto\ln s$, the corresponding f_2 instead of being zero, grows like $(\ln s)^2$. So as the energy increases, the apparent positive-correlation effect becomes stronger and stronger.

The second effect is due to the emission of clusters (or resonances), which decay into two or more pions.[2] In general, the more pions in a cluster, the bigger is the correlation effect, and in turn, the larger is f_2. The third effect is due to the constraint of the conservation of charge.[3] For example, for a system which independently emits π^+, π^0, π^-, the quantity f_2^- is negative. This simply reflects the fact that once a negative pion is emitted, the probability for the emission of a second negative pion is less than that for an uncorrelated case.

The f_1^- and f_2^- data for pp collisions are illustrated in Fig. 1.[4] Using some typical diffractive component (to be discussed in Sec. III), we have obtained the quantities $f^-{}_{1\,\rm nd}$ and $f^-_{2\,\rm nd}$ for the nondiffractive component, which are also shown in Fig. 1. Note the nondiffractive component data has a large uncertainty. For $p_{\rm Lab}\gtrsim 50$ GeV/c, the data are compatible with, e.g., $f^-_{2\,\rm nd}\approx 0$. This possibility was considered, e.g., in Ref. 5. For this case, the negative-correlation effect due to the constraint of conservation of charge can be trivially "accounted for" by assuming the final-state pions are decay products of isoscalar mesons such as the σ, ω, f^0, etc., which are independently emitted. We shall refer to this scheme as an "isoscalar cluster model". It is unclear within this model, for instance, why pions are not emitted directly. Also aside from the 303-GeV/c data point, the $f^-_{2\,\rm nd}$ data points appear to have a small positive slope[6]; it is negative below 50 GeV/c and is positive, say, at 205 GeV/c. The indicative slope is ignored in this model. Furthermore, to our knowledge, no quantitative fits, based on this scheme to all multi-

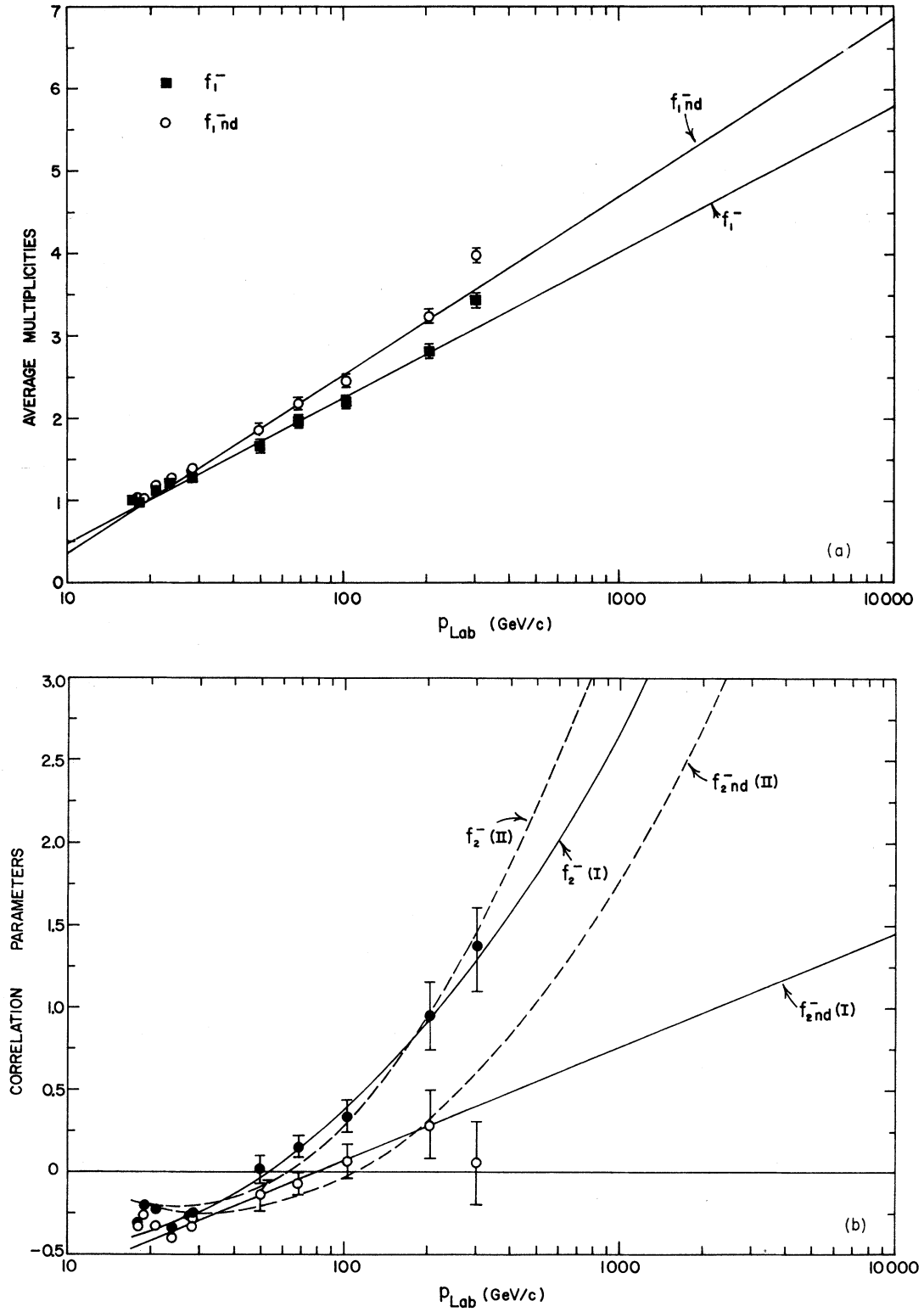

FIG. 1. Energy dependence of (a) the average multiplicities: f_1^- and f_{1nd}, and (b) the correlation parameters f_2^- and and f_{2nd}^-. Curves in 1(a) are $f_1^- = \lambda f_{1d}^1 + (1-\lambda) f_{1nd}^-$, $f_{1nd}^- = -1.80 + 0.94 \ln p_{Lab}$, with $\lambda = \sigma^d/\sigma_{in} \approx 0.18$ and $f_{1d}^- = 0.99$. Curves in 1(b) are: (I) $f_{2nd}^- \sim -1.32 + 0.30 \ln p_{Lab}$; (II) $f_{2nd}^- \sim 0.20(1 + f_{1nd}^-)^2 - f_{1nd}^-$ (see Ref. 17). The corresponding f_2^- are determined from Eq. (1.1). For the data used, see Ref. 4 and also Table II.

plicity data (especially the large-multiplicity data), have been obtained thus far.

In this note we would like to consider the possibility that at high enough energy the quantity $f_{2\,\mathrm{nd}}^{-}$ is, in fact, positive. For this alternative, the above simple model is inadequate. And as we shall see later, here the emission of clusters which contain at least one $\pi^-\pi^-$ pair in the final decay product is needed. The clusters could be resonances. The known prominent nonstrange resonances[7] up to $M \approx 1300$ MeV are tabulated in Table I. The ones having the desired $\pi^-\pi^-$ pair are A_1^-, A_2^-, and B^-. We shall see so far as the charge-multiplicity distribution is concerned the emission of *all* those resonances of Table I can be represented by the emission of π, σ, B "effective" resonances (or clusters). For quantitative fit to all available data, it turns out that the πB alone (πB scheme) are already adequate. In following sections we will consider models which involve the independent emission of the neutral and charge clusters. They are models where all the three correlation effects discussed are incorporated, giving predictions to charge-multiplicity distributions which differ from a Poisson distribution.

The main points of this work are the following:

(1) We discuss the formalism for the simultaneous emission of neutral and charge clusters.

(2) We present a simple two-component model compatible with the data based on the independent emission of clusters. The nondiffractive component is described by the independent emission of the π and the B clusters. From the $f_{1\,\mathrm{nd}}^{-}$ and $f_{2\,\mathrm{nd}}^{-}$ data, we find that the cluster-emission strength parameters are linear in $\ln p_{\mathrm{Lab}}$, which is expected from, for example, a multiperipheral model with both π and B independently emitted along the multiperipheral chain.

(3) Our model gives a good description to all available data from 18 GeV/c up, i.e., for both the charged pion multiplicity distribution,[4] and the π^0 average multiplicity versus fixed π^- number,[8] $\langle n_0 \rangle_-$ vs n_-. Our model is also compatible with the missing-mass data in single diffractive productions.[9]

(4) Our solution predicts an observable separation between the two components at around 1000–1500 GeV/c and an insignificant energy variation for the quantity $\langle n_0 \rangle_-$ between 200 to 1500 GeV/c.

The plan of our paper is as follows: In Sec. II, we discuss a general formalism for the independent emission of charge and neutral clusters. In Sec. III, we present a diffractive model based on cluster emission. In Sec. IV, we discuss the parameterization of the nondiffractive component and the two-component model. Also we present the cluster-emission parameters and compare our predictions with the charge and neutral data. We comment on the asymptotic predictions in Sec. V.

II. A GENERAL FORMALISM FOR THE INDEPENDENT EMISSION OF NEUTRAL AND CHARGED CLUSTERS

Formalism for independent emission of charged particles and clusters has been discussed extensively by different authors.[10] For completeness, we present here a simple generalization to earlier formalism, which now takes into account the simultaneous emission of neutral and charged clusters. Consider first the independent emission of an arbitrary number of various types of clusters from a neutral system. We label the "cluster type" by the charge state and the decay mode. For definiteness we consider only clusters which have the usual

TABLE I. Prominent $S=0$ mesons and their decay modes.

Mesons	$q=+1$ (charge)	h_+	$q=-1$	h_-	$q=0$	h_0
π	π^+	$c_\pi x$	π^-	$c_\pi y$	π^0	$c_\pi z$
ρ	$\rho^+ \to \pi^+\pi^0$	$c_\rho xz$	$\rho^- \to \pi^-\pi^0$	$c_\rho yz$	$\rho^0 \to \pi^+\pi^-$	$c_\rho xy$
ω					$\omega \to \pi^+\pi^-\pi^0$	$c_\omega xyz$
$\sigma(f^0)$					$\sigma \to \pi^+\pi^-$	$2c_\sigma xy$
					$\sigma \to \pi^0\pi^0$	$c_\sigma z^2$
$A_2(A_1)$	$A_2^+ \to \pi^+\pi^0\pi^0$	$c_A xz^2$	$A_2^- \to \pi^-\pi^0\pi^0$	$c_A yz^2$	$A_2^0 \to \pi^+\pi^-\pi^0$	$2c_A xyz$
	$A_2^+ \to \pi^+\pi^+\pi^-$	$c_A x^2 y$	$A_2^- \to \pi^-\pi^-\pi^+$	$c_A xy^2$		
B	$B^+ \to \pi^+\pi^+\pi^-\pi^0$	$c_B x^2 zy$	$B^- \to \pi^+\pi^-\pi^-\pi^0$	$c_B xy^2 z$	$B^0 \to \pi^+\pi^-\pi^0\pi^0$	$c_B xyz^2$

nonexotic quantum number. The generalization to more complicated cases is straightforward. Let the decay modes of arbitrary charged and neutral clusters be

$$C_i^+ \to (q_i+1)\pi^+ + q_i\pi^- + p_i\pi^0,$$

$$C_j^- \to q_j\pi^+ + (q_j+1)\pi^- + p_j\pi^0,$$

$$C_k^0 \to q_k\pi^+ + q_k\pi^- + p_k\pi^0.$$

The probability for the simultaneous emission of a number N_i^+ (N_j^-, N_k^0) of clusters C_i^+ (C_j^-, C_k^0) for a certain set of $[i,j,k]$ is

$$P([N_i^+],[N_j^-],[N_k^0]) = \prod_{[i]} \frac{c_i^{N_i^+}}{N_i^+!} \prod_{[j]} \frac{c_j^{N_j^-}}{N_j^-!} \prod_{[k]} \frac{c_k^{N_k^0}}{N_k^0!} \Big/ e^{h_0} I_0(2(h_+h_-)^{1/2}), \tag{2.1}$$

where $h_+ = \sum_{[i]} c_i$, etc., and c_i (c_j, c_k) is the parameter which specifies the strength for the emission of the cluster C_i^+ (C_j^-, C_k^0). We will refer it as the "cluster-emission strength parameter", or the "emission parameter" for short. Conservation of charge requires $\sum_{[i]} N_i^+ = \sum_{[j]} N_j^-$. The grand generating function for the final-pion multiplicity distribution is given by

$$G(x,y,z) = \sum_{n,m} \sigma_{nm}(xy)^n z^m/\sigma = \sum_{[N_i^+, N_j^-, N_k^0]} \prod_{[i]} \frac{[c_i(x,y,z;+)]^{N_i^+}}{N_i^+!} \times \prod_{[j]} \frac{[c_j(x,y,z;-)]^{N_j^-}}{N_j^-!} \times \prod_{[k]} \frac{[c_k(x,y,z;0)]^{N_k^0}}{N_k^0!}, \tag{2.2}$$

with

$$c_i(x,y,z;+) = c_i x (xy)^{q_i} z^{p_i}, \qquad c_j(x,y,z;-) = c_j y (xy)^{q_j} z^{p_j}, \tag{2.3}$$

and

$$c_k(x,y,z;0) = c_k (xy)^{q_k} z^{p_k}.$$

The summation is over $N_i^+, N_j^-, N_k^0 = 0, 1, 2, \ldots, \infty$ for all $[i]$, $[j]$, and $[k]$. We have ignored the constraint of conservation of energy. This is a good approximation at high energy, since the average multiplicity of the clusters grows at most like $\ln s$, while the total available energy grows like $\sqrt{s}$. We assign the total number of negative (neutral) clusters emitted to be n (m). After summing over the various terms and making use of a Bessel function identity,[11] we get

$$G(x,y,z) = \sum_{n,m} \frac{h_0^m(x,y,z)[h_+(x,y,z)h_-(x,y,z)]^n}{m!\,n!\,n!} \Big/ e^{h_0} I_0(2(h_+h_-)^{1/2}) = \frac{\exp[h_0(x,y,z)-h_0] I_0(2[h_+(x,y,z)h_-(x,y,z)]^{1/2})}{I_0(2(h_+h_-)^{1/2})}, \tag{2.4}$$

where

$$h_+(x,y,z) = \sum_{[i]} c_i(x,y,z;+), \qquad h_-(x,y,z) = \sum_{[j]} c_j(x,y,z;-), \tag{2.5}$$

and

$$h_0(x,y,z) = \sum_{[k]} c_k(x,y,z;0).$$

The multiplicity distributions for negative-charge, charged, and neutral pions can be obtained by expanding Eq. (2.4) in power series of y, xy, and z, respectively and comparing it to Eq. (2.2). In terms of the complete set of the negative-charge correlation parameters f_i^-, the grand generating function as usual can be written as

$$G(1,y,1) = G(1,1,1)\exp\left[\sum_{n=1}^{\infty} \frac{(y-1)^n f_n^-}{n!}\right]. \tag{2.6}$$

The parameters f_i^- can be calculated from Eq. (2.4) in the usual manner,

$$f_i^- = \frac{\partial^i}{\partial y^i} \ln G(x,y,z)\Big|_{x=y=z=1}. \tag{2.7}$$

Similar expressions for charged and neutral correlation parameters can also be written.

For the independent emission of a given type of isoscalar clusters,

$$f_1^- = cq, \quad f_2^- = cq(q-1), \tag{2.8}$$

and for isovector clusters,

$$f_1^- = c(2q+1)\frac{I_0'}{I_0} + cq \tag{2.9}$$

and

$$f_2^- = c\left[q(q-1) + \tfrac{1}{2}(2q+1)(2q-1)\frac{I_0'}{I_0}\right] + (2q+1)^2 c^2\left[\frac{I_0''}{I_0} - \left(\frac{I_0'}{I_0}\right)^2\right], \quad (2.10)$$

where I_0' and I_0'' are the first and the second derivatives of the modified Bessel function $I_0 \equiv I_0(2c)$, and the subscripts and superscripts are dropped for simplicity. From Eqs. (2.6), (2.7), and (2.8) and Table I, it is a straightforward matter to check that the parameter f_2^- for the emission of any of the π, ρ, σ, ω, or f^0 mesons is either negative or zero. This is due to the fact that there is at most one π^- in their decay modes. On the other hand, A_1^-, A_2^-, and B^- have $\pi^-\pi^-$ pair in the final decay product, and one finds that the corresponding f_2^- for the emission of A_1, A_2, or B is positive. Also so far as the negative-charge multiplicity is concerned one can easily check that associated with the emission of all resonances of Table I, only the following three linear combinations of the emission parameters appear:

$$c_\pi + c_\rho + c_{A1} + c_{A2}, \quad c_{A1} + c_{A2} + c_B, \quad \text{and} \quad c_\rho + c_\omega + 2c_\sigma + c_f + 2(c_{A1} + c_{A2}) + c_B. \quad (2.11)$$

Thus without loss of generality, we can choose the effective resonances or clusters to be the π, σ, and B.

So far we have considered independent cluster emission from a neutral excited system. For an excited system with net charge Q, the grand generating function is identical to Eq. (2.2), except that the charge-conservation constraint is now replaced by $\sum_{[i]} N_i^+ - \sum_{[j]} N_j^- = Q$. Summing over the various terms, we get[3]

$$G = \left(\frac{x}{y}\right)^{Q/2} \frac{\exp[h_0(x,y,z)]\, I_Q(2[h_+(x,y,z)h_-(x,y,z)]^{1/2})}{\exp(h_0) I_Q(2(h_+h_-)^{1/2})} \equiv \sum_{n,m} \sigma_{n+Q,n,m} x^{n+Q} y^n z^m/\sigma, \quad (2.12)$$

with $\sigma = \sum_{n,m} \sigma_{n+Q,n,m}$, where I_Q is the Qth-order modified Bessel function of the first kind. Finally, if one makes a usual "statistical ansatz" assuming an equal weight to each possible isospin final state for all $I=1$ grand clusters emitted,[12] this together with the conservation of isospin leads to additional isospin weight factors present in Eq. (2.2). In particular, the generating function for this case is

$$G(x,y,z) = e^{h_0'(x,y,z)} \sum_{n,m} \frac{[h_0(x,y,z)]^m [h_+(x,y,z)h_-(x,y,z)]^n}{m!\,n!\,n!} \times [p^{(0)}_{n,m,n} + p^{(1)}_{n,m,n} + p^{(2)}_{n,m,n}], \quad (2.13)$$

where h_0' corresponds to isoscalar contribution, h_0 and $h_\pm$ to isovector contribution, and the $p^{(I)}$'s are the isospin weight factors specified in Eq. (15) of Ref. 12. We have checked that our conclusions are insensitive to these factors. For simplicity, we will not explicitly include these extra factors for the results presented in Sec. IV.

III. THE DIFFRACTIVE COMPONENT

Evidence for the presence of the diffractive component is mainly from the missing-mass spectra in single diffractive production. In the spectra for the 2-, 4-, and 6-prong events, one finds a low-mass enhancement, which is attributed to single diffractive-dissociation events.[9] Unfortunately, the missing-mass data have large uncertainties. We have chosen a typical diffractive component, which satisfies the following two criteria: First, it is compatible with the missing-mass information, and second it enables us within our model to get a consistent fit to all available charge-multiplicity data. Our diffractive component thus obtained (to be presented later) turns out to be also of the same order of magnitude as those considered by previous authors.[5,6] So our values are also a typical assessment of the diffractive component for present data.

Next we turn to the parametrization for the diffractive component. We also make use of the cluster-emission picture here. Since the average multiplicity for the diffractive component is small (typically $f_{1d}^- \sim 1$), we choose to parametrize this component by the independent emissions of the π and σ (the $\pi\sigma$ scheme). The generating function of pion multiplicities for diffractive dissociation at either the target side or the projectile side is given by

$$g(x,y,z) = \lambda_1 \frac{e^{c_1 z + c_2(2xy+z^2)} I_0(2(xy)^{1/2}c_1) - 1}{e^{c_1+3c_2} I_0(2c_1) - 1}, \quad (3.1)$$

with $\lambda_1 = \sqrt{\sigma^{dd}}$, where σ^{dd} is the cross section for the double diffractive dissociation. The numerator represents the contribution from the emission of π and σ (with their emission parameters c_1 and c_2) less an elastic scattering contribution. Assuming factorization, the unnormalized generating function for the diffractive component is given by

$$G^d(x,y,z) = [g(x,y,z) + \lambda_2]^2 - \lambda_2^2, \quad (3.2)$$

with that for the single diffraction component given by $G^{sd} = 2\lambda_2 g(x,y,z)$. The quantity in the bracket describes the emission from either of the two excited systems including the elastic scattering contribution. The parameter $\lambda_2^2 = \sigma_{el}$. The total dif-

fractive cross section, which is the sum of the single and the double diffractive production cross section, is given by

$$\sigma^{d}=\sigma^{sd}+\sigma^{dd}, \tag{3.3}$$

with $\sigma^{sd}=2\lambda_1\lambda_2$ and $\sigma^{dd}=\lambda_1^{2}$. Expanding Eqs. (3.1) and (3.2) we get[13]

$$\sigma_0^{d}(z)=[\Lambda(e^{c_1z+c_2z^2}-1)+\lambda_2]^2-\lambda_2^{2}, \tag{3.4}$$

$$\sigma_{n_-}^{d}(z)=2(\lambda_2-\Lambda)\Lambda e^{c_1z+c_2z^2}\left[\sum_{n=0}^{n_-}\frac{(2c_2)^{n_--n}c_1^{2n}}{(n_--n)!\,n!\,n!}\right]$$
$$+(\Lambda e^{c_1z+c_2z^2})^2\left[\sum_{n=0}^{n_-}\frac{(4c_2)^{n_--n}c_1^{2n}(2n)!}{(n_--n)!\,(n!)^4}\right]$$
$$(n_->0); \tag{3.5}$$

$$\sigma_0^{sd}(z)=2\lambda_2\Lambda[e^{c_1z+c_2z^2}-1], \tag{3.6}$$

$$\sigma_{n_-}^{sd}(z)=2\lambda_2\Lambda e^{c_1z+c_2z^2}\left[\sum_{n=0}^{n_-}\frac{(2c_2)^{n_--n}c_1^{2n}}{(n_--n)!\,n!\,n!}\right],$$
$$n_->0 \tag{3.7}$$

where

$$\Lambda=\sigma^{sd}/\{2\lambda_2[e^{c_1+3c_2}I_0(2c_1)-1]\}. \tag{3.8}$$

In the above expressions we have included explicitly the z dependence for later convenience; $\sigma_{n_-}^{d}=\sigma_{n_-}^{d}(1)$, $\sigma_{n_-}^{sd}=\sigma_{n_-}^{sd}(1)$.

The diffractive component in this model is specified by three parameters. With the criteria given earlier, we found

$$\sigma^{sd}=5.0\ \text{mb},\qquad c_1=0.544,\quad c_2=0.194, \tag{3.9}$$

where we have assumed[14] $\sigma^{el}=6.9$ mb, which leads to $\sigma^{d}=5.9$ mb. With the parameters obtained, the corresponding average multiplicity and the correlation parameter are given by

$$f_{1d}^{-}=0.99,\quad f_{2d}^{-}=-0.16. \tag{3.10}$$

For completeness, we give in Table II the single diffractive and the total diffractive negative-charge multiplicity distributions predicted by Eq. (3.9). They are also shown in Fig. 5.

TABLE II. The diffractive-component π^- multiplicity distribution.

n_-	$\sigma_{n_-}^{sd}$ (mb)	$\sigma_{n_-}^{d}$ (mb)
0	1.78	1.89
1	2.33	2.63
2	0.72	1.02
3	0.141	0.282
4	0.020	0.065
5	0.002	0.013

IV. A TWO-COMPONENT MODEL BASED ON CLUSTER EMISSION AND THE DATA

A. The Nondiffractive Component Parametrization

We mentioned earlier that the most general parametrization for the π^- multiplicity distribution due to the emission of resonance of Table I can be represented by the $\pi B\sigma$ scheme. It turns out that the nondiffractive-component data can be adequately fitted by the πB scheme alone. For brevity we shall only present the parametrization for the πB scheme. The generalization to other cases is straightforward.

Denote the emission parameters for the π and B by c_1 and c_2, respectively. From Table I, we get

$$h_+(x,y,z)=(c_1+c_2xyz)x,$$
$$h_-(x,y,z)=(c_1+c_2xyz)y,$$
$$h_0(x,y,z)=(c_1+c_2xyz)z. \tag{4.1}$$

and

And from Eq. (2.4), the corresponding generating function for the pion multiplicity distribution is given by

$$G^{nd}(x,y,z)=\frac{e^{(c_1+xyzc_2)z}I_0(2(xy)^{1/2}(c_1+c_2xyz))}{e^{c_1+c_2}I_0(2c_1+2c_2)}$$
$$=\sum_{n_-}\sigma_{n_-}^{nd}(z)(xy)^{n_-}/\sigma^{nd}. \tag{4.2}$$

Furthermore,

$$f_{1nd}^{-}=c_2+(c_1+3c_2)\frac{I_0'}{I_0} \tag{4.3}$$

and

$$f_{2nd}^{-}=(c_1+3c_2)^2\left[\frac{I_0''}{I_0}-\left(\frac{I_0'}{I_0}\right)^2\right]+\tfrac{1}{2}(-c_1+3c_2)\frac{I_0'}{I_0}, \tag{4.4}$$

where the argument of I_0, I_0', and I_0'' is $2(c_1+c_2)$.

With the f_{1nd}^{-} and f_{2nd}^{-} data shown in Fig. 1, from Eqs. (4.3) and (4.4) we have solved the parameters c_1 and c_2 numerically. The obtained quantities c_1 and $4c_2$ are shown in Fig. 2. Notice that in the low-energy region, $c_1\gg 4c_2$ and the pions are mainly from direct emission. When $c_1=4c_2$, half of the pions in the nondiffractive component are from direct emission and half from B clusters. This occurs at around 140 GeV/c. As the energy increases further, apparently more and more pions come from the B cluster. This plot thus shows quantitatively the increase of the clustering effect (the emission of clusters) as the energy

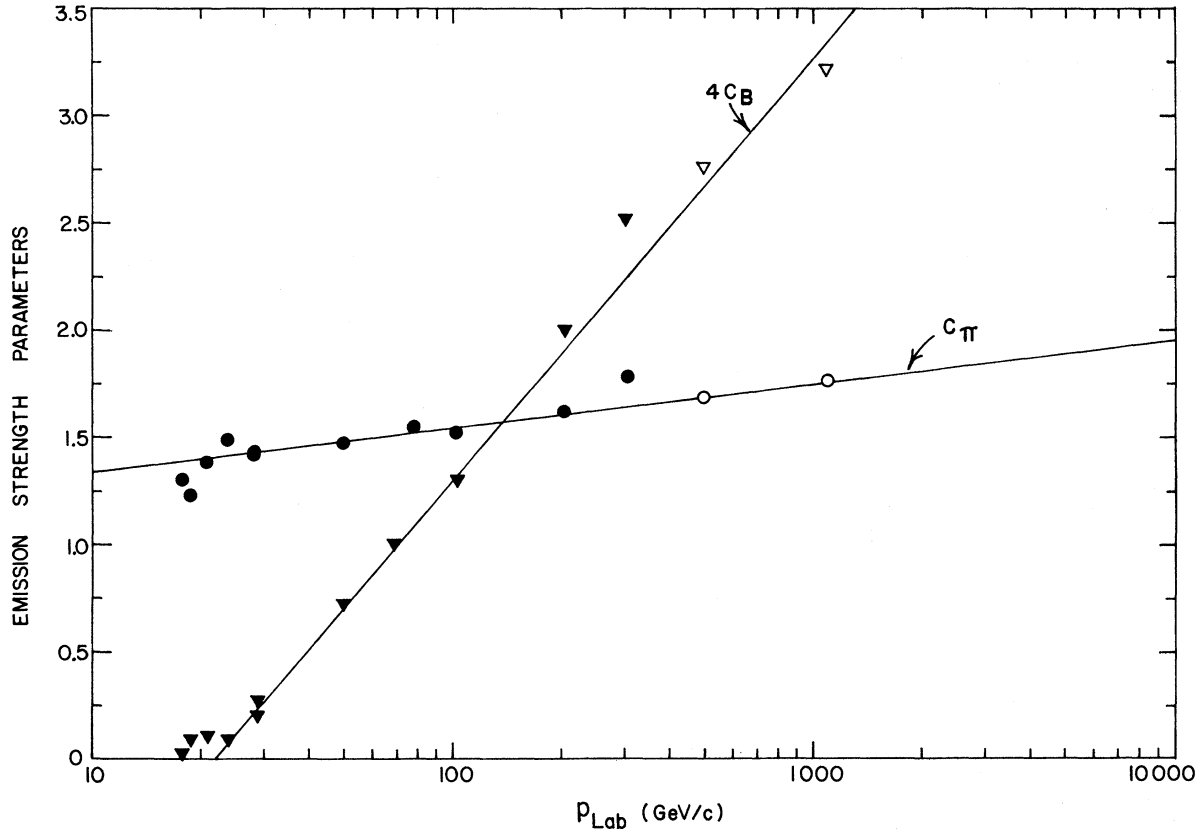

FIG. 2. Energy dependence of the cluster-emission strength parameters. Solid points are determined from the experimental $f_{1\text{nd}}^-$ and $f_{2\text{nd}}^-$ values and open points are determined from the linear extrapolation shown in Fig. 1. Parameters for the linear fits are given in Eq. (4.5).

increases. The cluster emission parameters are approximately linear in $\ln p_{\text{Lab}}$. The lines illustrated correspond to

$$c_1 \sim 0.088 \ln p_{\text{Lab}} + 1.14$$

and (4.5)

$$4c_2 \sim 0.86 \ln p_{\text{Lab}} - 2.66 .$$

This linearity in $\ln p_{\text{Lab}}$ is characteristic of, for example, the multiperipheral model where the π and the B are independently emitted along the multiperipheral chain.[15] From Eqs. (4.3) and (4.4) and the asymptotic behavior of the Bessel function, for large c_1 and c_2,

$$f_{1\text{nd}}^- \to c_1 + 4c_2 , \quad f_{2\text{nd}}^- \to -\tfrac{1}{2}c_1 + \tfrac{3}{2}c_2 . \tag{4.6}$$

From Eqs. (4.5) and (4.6), keeping only the $\ln p_{\text{Lab}}$ term, we get

$$f_{1\text{nd}}^- \sim 0.95 \ln p_{\text{Lab}} , \quad f_{2\text{nd}}^- \sim 0.28 \ln p_{\text{Lab}} . \tag{4.7}$$

The coefficients here are quite close to the experimental numbers (0.94 and 0.30, respectively) given in the caption of Fig. 1. This serves as an independent check for our calculation.

B. The Charge-Multiplicity Distribution

To obtain the nondiffractive-component multiplicity distribution for the πB scheme, we expand Eq. (4.2) in powers of y and get

$$\sigma_{n_-}^{\text{nd}}(z) = \sigma^{\text{nd}} e^{c_1 z} c_2^{n_-} \sum_{n=0}^{n_-} \frac{(c_1^2/c_2)^n}{n!\,n!} \sum_{k=0}^{\min(n_- - n, 2n)} \frac{z^{2n_- - 2n - k}}{c_1^k (n_- - n - k)!} \binom{2n}{k} \Big/ [e^{c_1 + c_2} I_0(2c_1 + 2c_2)] , \tag{4.6'}$$

where $\binom{2n}{k}$ is the binomial coefficient and the distribution we are looking for is given by $\sigma_{n_-}^{\text{nd}} = \sigma_{n_-}^{\text{nd}}(1)$. The total inelastic cross section σ_{in} varies somewhat with energy,[4] $\sigma_{\text{nd}} = \sigma_{\text{in}} - \sigma_{\text{el}}$.

$$\sigma_{n_-} = \sigma^{\mathrm{nd}}_{n_-} + \sigma^{\mathrm{d}}_{n_-}, \tag{4.7'}$$

with $\sigma^{\mathrm{d}}_{n_-}$ being given in Eqs. (3.4) and (3.5). The predicted distributions using the obtained c_1 and c_2 points of Fig. 2 (for 303 GeV/c, the linear fits were used), together with the data[4] are shown in Fig. 3. The agreement between the predictions and the data is reasonable.

C. The $\langle n_0\rangle_-$ vs n_- Data

For the nondiffractive component

$$\langle n_0\rangle^{\mathrm{nd}}_- = \frac{d}{dz}\ln\sigma^{\mathrm{nd}}_{n_-}(z)\bigg|_{z=1}, \tag{4.8}$$

where $\sigma^{\mathrm{nd}}_{n_-}(z)$ is given in Eq. (4.6). After some algebra we get

$$\langle n_0\rangle^{\mathrm{nd}}_- = c_1 + \frac{e^{c_1}}{\sigma^{\mathrm{nd}}_{n_-}} \sum_{n=0}^{n_-} \frac{(c_1^2/c_2)^n}{n!\,n!} \times \sum_{k=0}^{\min(n_- - n, 2n)} \frac{(2n_- - 2n - k)}{c_1^{\,k}(n_- - n - k)!} \binom{2n}{k}. \tag{4.9}$$

The final $\langle n_0\rangle_-$ value in our two-component model is given by

$$\langle n_0\rangle_- = \lambda\langle n_0\rangle^{\mathrm{d}}_- + (1-\lambda)\langle n_0\rangle^{\mathrm{nd}}_-, \tag{4.10}$$

where $\langle n_0\rangle^{\mathrm{nd}}_-$ is given in Eq. (4.9) with $\lambda = \sigma^{\mathrm{d}}/(\sigma^{\mathrm{d}}+\sigma^{\mathrm{nd}})$, while

$$\langle n_0\rangle^{\mathrm{d}}_- = \frac{d}{dz}\ln\sigma^{\mathrm{d}}_{n_-}(z)\bigg|_{z=1}, \tag{4.11}$$

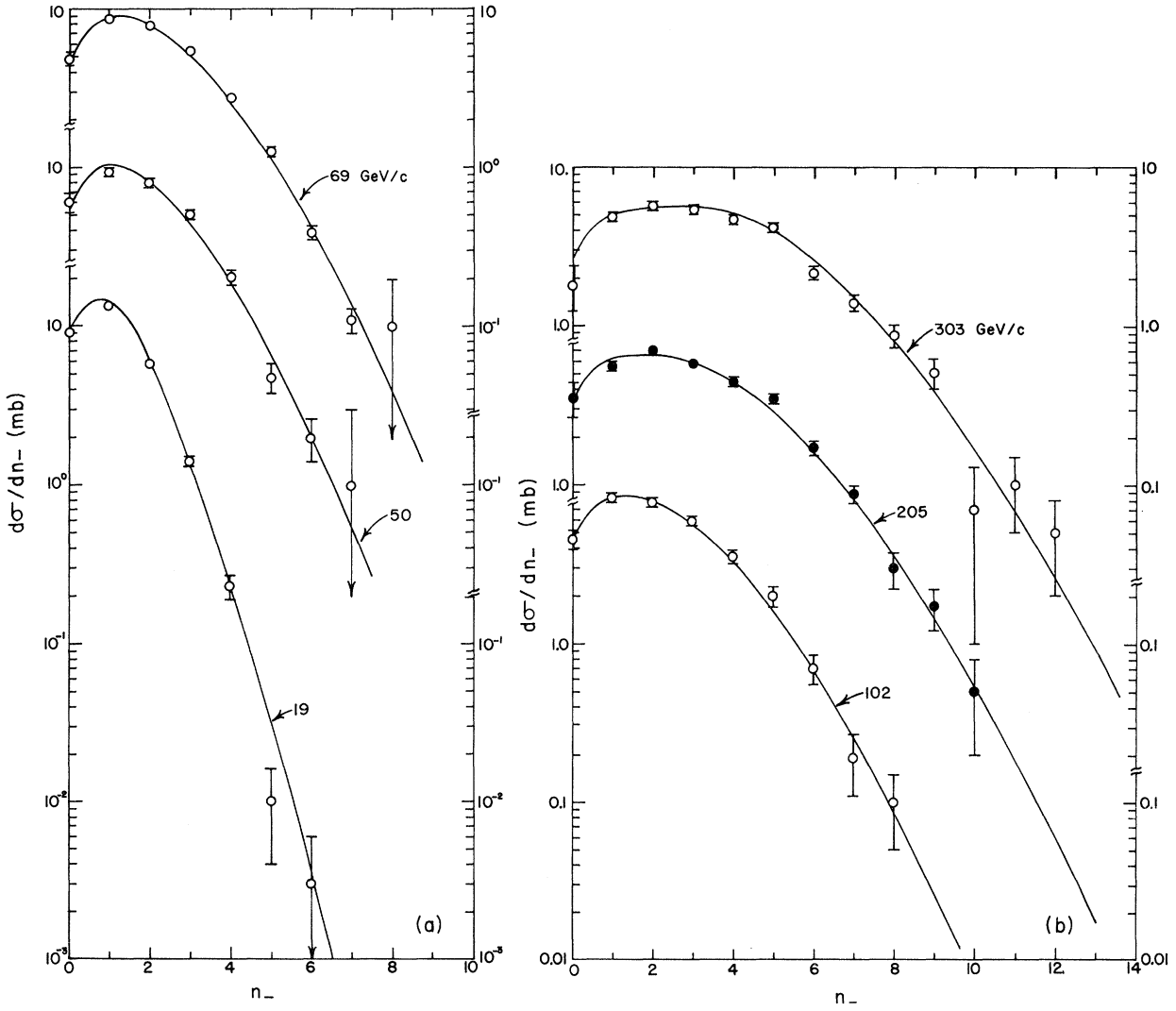

FIG. 3. A comparison on the charge-multiplicity distribution between the predictions of the two-component cluster emission model of Sec. IV and the data. For data points used, see Ref. 4.

with $\sigma^{d}_{n_-}(z)$ given in Eqs. (3.4) and (3.5). The data[8] at 19 GeV/c and at 205 and 303 GeV/c together with our predictions are shown in Fig. 4. The agreement between the data and the prediction again appears to be reasonable, although the data are not very accurate and they do not provide a stringent test to the model.

V. DISCUSSION

We have presented a simple model which has incorporated all the three factors mentioned in the Introduction giving rise to the different correlation effect. In particular it is a two-component model based on independent emission of neutral and charged clusters, which takes into account the effect of conservation of charge. The obtained cluster-emission strength parameters shown in Fig. 3 imply that the clustering phenomena (i.e., the emission of clusters), in the presence of a significant direct-pion emission, become more and more important as the energy increases. This conclusion is not only peculiar to the πB scheme considered. We have also looked at the corresponding situation for the πA_2 scheme and also the $\pi B\sigma$ scheme (for the latter case the $\langle n_0\rangle_-$ data at $n_-=0$ was also used as an additional input for solving c_π, c_B, and c_σ). Similar clustering effects are also observed for both schemes, although for the $\pi B\sigma$ case due to the presence of the σ contribution, the emission parameter for B is somewhat reduced compared to that for the πB scheme. We have also compared the nondiffractive-component multiplicity distribution for cases both with and without the isospin weight factors of Eq. (2.13). Our conclusion on the clustering effect is again insensitive to this variation.

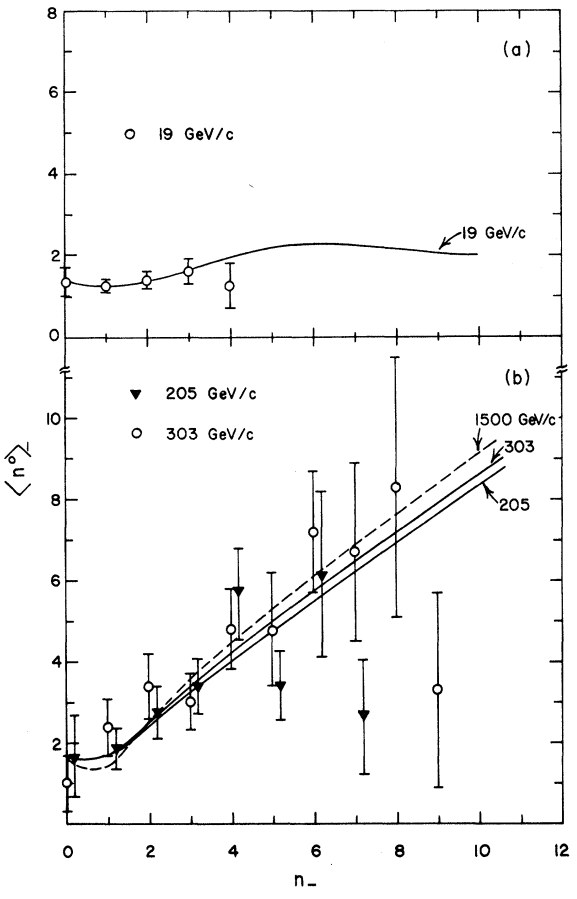

FIG. 4. A comparison on the neutral data: $\langle n_0\rangle_-$ vs n_-, between the prediction of the two-component cluster-emission model and the data. For data points, see Ref. 8. The dashed curve is the prediction at 1500 GeV/c based on the linear extrapolations for both $f^{-}_{1\mathrm{nd}}$ and $f^{-}_{2\mathrm{nd}}$ shown in Fig. 1.

Our model suggests the following cluster-emission picture for the nondiffractive-component multiparticle production: For $p_{\mathrm{Lab}} \approx 20$ GeV/c, the independent emission of pions dominates. There, as expected from the constraint of conservation of charge, $f^{-}_{2\mathrm{nd}} < 0$. As the energy increases, the emission of σ, ρ, and ω also becomes significant with $f^{-}_{2\mathrm{nd}}$ still being negative. Later on at higher energies, the clusters such as the A_2, A_1, and B also participate. Eventually these last clusters dominate and the $f^{-}_{2\mathrm{nd}}$ becomes positive. Empirically, such a relatively complicated picture can be accounted for by the πB scheme with the πB emission parameters both being linear in $\ln p_{\mathrm{Lab}}$, in reminiscence of the prediction of a multiperipheral model.[15] If the $f^{-}_{1\mathrm{nd}}$ and $f^{-}_{2\mathrm{nd}}$ data are extrapolated linearly in $\ln p_{\mathrm{Lab}}$ to higher energy, the corresponding c_1 and c_2 will continue to rise linearly in $\ln p_{\mathrm{Lab}}$. The predicted charge-multiplicity distributions at 500, 1000, and 1500 GeV/c with such an extrapolation is shown in Fig. 5. Notice that at around 1000–5000 GeV/c the separation between the diffractive and the nondiffractive components is already noticeable. The corresponding high-energy prediction at 1500 GeV/c for $\langle n_0\rangle_-$ is shown in Fig. 4. Apparently this quantity is insensitive to the energy variation considered.

To contrast to the predicted charge-multiplicity distribution, in Fig. 5 we also show the corresponding prediction from a quadratic extrapolation to the $f^{-}_{2\mathrm{nd}}$ data [i.e., $f^{-}_{2\mathrm{nd}} \propto (\ln s)^2$, see Fig. 1(b)]. This extrapolation has been discussed in the context of KNO-scaling behavior[16] for the nondiffractive multiplicity distribution in Ref. 17. Even at 1000–1500 GeV/c the two predictions do not differ significantly from each other, although for the case with $f^{-}_{2\mathrm{nd}} \propto (\ln s)^2$, the separation between the

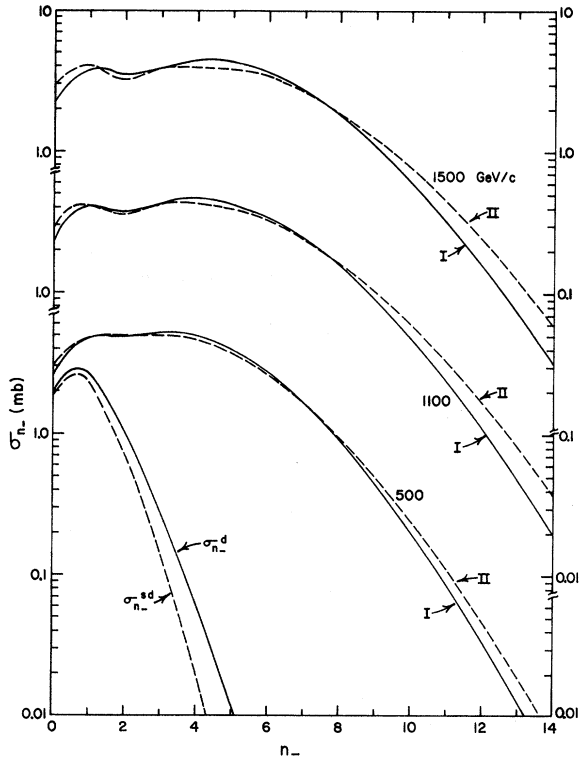

FIG. 5. Predictions for the negative-charge pion multiplicity distribution at 500, 1100, and 1500 GeV/c. The solid curves correspond to extrapolation I for the $f_{2\text{nd}}^{-}$ and the dashed curves correspond to extrapolation II for $f_{2\text{nd}}^{-}$. The total diffractive component $\sigma_{n}^{d}{}_{-}$ and the single diffractive component $\sigma_{n}^{sd}{}_{-}$ chosen are illustrated in the lower portion of the figure.

diffractive and nondiffractive components appears to be more pronounced beyond 1000 GeV/c and also the corresponding $f_{2\text{nd}}^{-}$ is significantly larger than that for the $f_{2\text{nd}}^{-} \propto \ln s$ case [see Fig. 1(b)]. Future experiments on energy dependence of the $f_{2\text{nd}}^{-}$ and the observation of the two-component separation are needed to distinguish between the different proposals. If $f_{2\text{nd}}^{-} \propto (\ln s)^2$ turns out to be favored by higher-energy data, this would imply that the pion content of clusters will have to grow as the energy further increases. We have also looked at the prediction for the neutral data: $\langle n_0 \rangle_-$ vs n_-. There is not much variation from 205 GeV/c to 1500 GeV/c. It is of interest to see if future data support this prediction.

Added note. After the completion of the present paper, a question was raised as to whether this work can be used to discriminate between the multiperipheral model and the fragmentation model. We have since calculated the topological distribution for the multiperipheral model using, e.g., the "I model" of Caneschi and Schwimmer[18] with a modification to allow the emission of both pions and B clusters. The distribution obtained is similar to the nondiffractive component distribution presented in this paper. Furthermore, in Ref. 17, we have explicitly compared the topological distribution from one excited fragment, which subsequently decays through independent emission, and that from two excited fragments. We found that these two distributions with the appropriate adjustment of parameters can be made very similar. Thus, at the level of topological cross sections, with the available information, it is unlikely that one can discriminate between the multiperipheral model and the fragmentation model.

ACKNOWLEDGMENTS

One of us (CBC) would like to thank Dr. M. Jacob and Dr. D. Tow for discussions on two-component models. We also wish to thank Dr. P. Slattery and Dr. B. Y. Oh for discussions on their data.

---

*Work supported in part by the U. S. Atomic Energy Commission under contract No. (40-1) 3992.

[1]K. Wilson, Cornell University Report No. CLNS 131, 1970 (unpublished). See also M. Jacob, in *Proceedings of the XVI International Conference on High Energy Physics, Chicago-Batavia, Ill., 1972,* edited by J. D. Jackson and A. Roberts (NAL, Batavia, Ill., 1973), Vol. 3, p. 373. See also references quoted therein.

[2]W. R. Frazer, R. D. Peccei, S. S. Pinsky, and C.-I Tan, Phys. Rev. D 7, 2647 (1973); C. J. Hamer, Phys. Rev. D 7, 2723 (1973).

[3]For models of independent emission of charged particles, see, for example, H. A. Kastrup [Nucl. Phys. B1, 309 (1967)], and D. Horn and R. Silver [Phys. Rev. D 2, 2082 (1970)].

[4]The negative-charge multiplicity data in pp collisions used are as follows:

(a) 19 GeV/c: H. Bøggild *et al.*, Nucl. Phys. B27, 285 (1971);

(b) 18, 21, 24, and 28.5 GeV/c: D. B. Smith *et al.*, Phys. Rev. Lett. 23, 1064 (1969); E. L. Berger, B. Y. Oh, and G. A. Smith, *ibid.* 29, 675 (1972); also private communication from B. Y. Oh and G. A. Smith, 1973;

(c) 28.5 GeV/c: W. H. Simms *et al.*, Nucl. Phys. B41, 317 (1972);

(d) 50 and 69 GeV/c: V. V. Ammosov *et al.*, Phys. Lett. 42B, 519 (1972);

(e) 102 GeV/c: J. W. Chapman *et al.*, Phys. Rev. Lett. 29, 1686 (1972);

(f) 205 GeV/c: G. Charlton *et al.*, *ibid.* 29, 515 (1972);

(g) 303 GeV/c: F. T. Dao *et al.*, *ibid.* 29, 1627 (1972).

[5]C. Quigg and J. D. Jackson, NAL Report No. NAL-THY-93, 1972 (unpublished): K. Fiałkowski and H. I. Miettinen, Phys. Lett. 43B, 61 (1973).
[6]This possibility was also considered, for example, in H. Harari and E. Rabinovici, Phys. Lett. 43B, 49 (1973).
[7]Particle data group, Phys. Lett. 39B, 1972.
[8]The neutral data, $\langle n_0 \rangle_-$ vs n_-:
(a) 19 GeV/c: H. Bøggild *et al.*, Nucl. Phys. B27, 285 (1971) (the data points used were taken from E. L. Berger *et al.* of Ref. 10);
(b) 205 GeV/c: G. Charlton *et al.*, Phys. Rev. Lett. 29, 1759 (1972);
(c) 303 GeV/c: F. T. Dao *et al.*, NAL-UCLA collaboration report, 1973 (unpublished).
[9]Missing-mass spectral data in single diffractive production. For 102-GeV/c pp data, see C. M. Bromberg *et al.*, [Rochester-Michigan Collaboration, University of Rochester Report No. UR 416, 1973 (unpublished)]. Similar spectra have also been reported at 205 and 303 GeV/c. See the proceedings of the Vanderbilt Conference, Vanderbilt University, Nashville, Tenn., March, 1973.
[10]See, for example, C. P. Wang, Phys. Rev. 180, 1463 (1969); B. R. Webber, Nucl. Phys. B43, 541 (1972); E. L. Berger, D. Horn, and G. H. Thomas, Phys. Rev. D 7, 1412 (1973); and also references quoted therein. See also Ref. 3.
[11]Bateman Manuscript Project, *Higher Transcendental Functions*, edited by A. Erdélyi (McGraw-Hill, New York, 1953), Vol. II, Sec. 7.10.1, Eq. (16).
[12]F. Cerulus, Nuovo Cimento 19, 528 (1961).
[13]In expanding the product of two Bessel functions, use has been made of a decomposition formula [see Ref. 11, Sec. 7.2.8, Eq. (48)].
[14]The elastic cross section assumed is taken from the 102-GeV/c data of Ref. 4, beyond which σ_{el} is approximately constant. In the lower-energy region the elastic cross section is somewhat larger. For example, $\sigma_{el} \sim 8.0 \pm 0.2$ mb at 24.6 GeV/c [see G. G. Beznogikh *et al.*, Phys. Lett. 39B, 411 (1972)]. Through factorization the corresponding single diffractive-dissociation contribution could be larger than the estimated value. Fortunately, owing to the large low-multiplicity cross sections (see Fig. 3), our underestimation on the diffractive component is unimportant here.
[15]D. Amati, A. Stanghellini, and S. Fubini, Nuovo Cimento 26, 896 (1962); G. F. Chew and A. Pignotti, Phys. Rev. 176, 2112 (1968). For a multiperipheral model with cluster emission, see H. Arbarbanel, Phys. Rev. D 6, 2788 (1972); see also Ref. 2.
[16]Z. Koba, H. B. Nielsen, and P. Olesen, Nucl. Phys. B40, 317 (1972).
[17]C. Chiu and K. H. Wang, CPT report, 1973 (unpublished).
[18]L. Caneschi and A. Schwimmer, Phys. Rev. D 3, 1588 (1971).

PHYSICAL REVIEW D VOLUME 8, NUMBER 9 1 NOVEMBER 1973

Proton Electromagnetic Form Factor—Data Analysis and Asymptotic Behavior

B. B. Deo and M. K. Parida
Physics Department, Utkal University, Bhubaneswar-4, Orissa, India
(Received 27 February 1973)

Existing data on the proton electromagnetic form factor are analyzed with a view to extrapolating to the vector-meson resonance region and also to suggesting a method of verifying bounds predicted by composite models. An N/D method is suggested. The D and the N functions are assumed to represent the elastic and inelastic cut contributions, respectively. We find that the existing data are consistent with the asymptotic behavior $[\ln Q^2]^c/(Q^2)^{(p+1)/2}$, with either $c = 4$, $p = 3$ or $c = 4$, $p = 5$. An unbiased extrapolation to the timelike region shows a resonance at $m_V = 708$ MeV having the width $\Gamma_V = 25$ MeV for the case $c = 4$, $p = 3$ and the resonance shifts to $m_V = 680$ MeV with $\Gamma_V = 120$ MeV for the case $c = 4$, $p = 5$. The latter fit extrapolates to the value $|G_M^p| = 0.25$ for $t = (2.1\ \text{GeV})^2$ compared with the Frascati datum point $|G_M^p| = 0.27 \pm 0.04$.

I. INTRODUCTION

A growing amount of experimental information on electromagnetic form factors at very high momentum transfer ($t = q^2 = -Q^2$) has spurred an increasing interest in the problem of finding an appropriate description of form factors in the asymptotic limit $Q^2 \to \infty$. There has been an extensive theoretical investigation of the asymptotic behavior of hadron form factors from the considerations of analyticity and consequent dispersion relations. A successful model has also been developed to calculate the hadron form factors by treating them as bound states in the ladder-approximation to the two-body Bethe-Salpeter equation. Both these types of investigations sometimes lead to different results. Experimental data on proton form factors based on some models seem to suggest that the nucleon is a composite particle, a bound state of a bare nucleon and a spinless scalar gluon. However, till now no definite analysis of data has been made to extract the